

Ab initio studies of electric transport in terms of the real space Kubo-Greenwood equation

K. Palotás,¹ B. Lazarovits,¹ L. Szunyogh,^{1,2} and P. Weinberger¹

¹Center for Computational Materials Science, Technical University Vienna, A-1060, Gumpendorferstr. 1.a., Vienna, Austria

²Department of Theoretical Physics and Center for Applied Mathematics and Computational Physics, Budapest University of Technology and Economics, Budafoki út 8., H-1521 Budapest, Hungary

(Received 17 June 2002; revised manuscript received 6 January 2003; published 8 May 2003)

We propose a method suitable to describe electrical transport properties of nanostructures. In this approach a Green's function embedding technique based on the fully relativistic spin-polarized Korringa-Kohn-Rostoker method and the coherent potential approximation is combined with a real-space formulation of the Kubo-Greenwood equation. We present calculations for the Ag(100) surface, Ag bulk, two types of CuPt bulk alloys in the "large cluster" limit as well as finite Fe and Co chains embedded into the surface layer of Ag(100) in order to illustrate the reliability and applicability of this approach.

DOI: 10.1103/PhysRevB.67.174404

PACS number(s): 75.30.Gw, 75.70.Ak, 75.70.Cn

INTRODUCTION

Magnetic nanostructures on surfaces are of special interest for the production of high-density magnetic recording devices. It is therefore an important issue to investigate the magnetic and electrical transport properties of such structures.^{1,2} The fully relativistic screened Korringa-Kohn-Rostoker Green's function method has been successfully applied in the past to layered systems (systems with two-dimensional translational symmetry) and reliable results have been provided for the magnetic properties of such systems.³⁻⁵ This approach was then extended in terms of the coherent potential approximation (CPA), and, in order to describe electrical transport properties of such systems, the Kubo-Greenwood formula^{6,7} was reformulated using one-particle Green's functions.^{8,9} This combination of methods has been successfully applied to various disordered layered systems with the aim of investigating giant magnetoresistance effects¹⁰ as well as evaluating residual resistivities¹¹.

The purpose of the present work is to propose a method suitable to describe electrical transport properties of nanostructures. We use the so-called embedding technique¹² in order to describe the scattering properties of a specific region of a surface or bulk (called cluster) in combination with a real-space formulation of the Kubo-Greenwood equation. In the present paper we are mainly concerned about the "large cluster" limit of transport properties in order to check the reliability of the proposed method. It should be noted, however, that this method is primarily designed to evaluate electric properties of mesoscopic clusters, nanodot or nanowire systems, etc. For this reason we investigated finite chains of Fe and Co embedded into the surface layer of Ag(100). In addition to this main goal, further theoretical challenges can be investigated such as the change of electric properties from a nanostructure scale to thin films or even bulk systems, as well as comparing for low dimensional disordered structures configurational averages in real space with CPA averages.^{8,13}

THEORETICAL APPROACH

Suppose the electrical conductivity of a disordered system, namely $\sigma_{\mu\nu}$, is calculated using the Kubo-Greenwood formula:^{6,7}

$$\sigma_{\mu\nu} = \frac{\pi\hbar}{N_0\Omega_{at}} \left\langle \sum_{m,n} J_{mn}^\mu J_{nm}^\nu \delta(\varepsilon_F - \varepsilon_m) \delta(\varepsilon_F - \varepsilon_n) \right\rangle. \quad (1)$$

In this equation $\mu, \nu \in \{x, y, z\}$, N_0 is the number of atoms, J^μ is a representation of the μ -th component of the current operator,

$$J_\mu = \{J_{nm}^\mu\}, \quad J_{nm}^\mu = \langle n | J_\mu | m \rangle, \quad (2)$$

ε_F is the Fermi energy, $|m\rangle$ an eigenstate of a particular configuration of the random system, Ω_{at} the atomic volume, and $\langle \dots \rangle$ denotes an average over configurations. Equation (1) can be reformulated in terms of the imaginary part of the (one-particle) Green's function

$$\sigma_{\mu\nu} = \frac{\hbar}{\pi N_0 \Omega_{at}} \text{Tr} \langle J_\mu \text{Im} G^+(\varepsilon_F) J_\nu \text{Im} G^+(\varepsilon_F) \rangle, \quad (3)$$

or, by using "up-" and "down-" side limits, this equation can be rewritten as

$$\sigma_{\mu\nu} = \frac{1}{4} \{ \tilde{\sigma}_{\mu\nu}(\varepsilon^+, \varepsilon^+) + \tilde{\sigma}_{\mu\nu}(\varepsilon^-, \varepsilon^-) - \tilde{\sigma}_{\mu\nu}(\varepsilon^+, \varepsilon^-) - \tilde{\sigma}_{\mu\nu}(\varepsilon^-, \varepsilon^+) \}, \quad (4)$$

where

$$\varepsilon^+ = \varepsilon_F + i\delta, \quad \varepsilon^- = \varepsilon_F - i\delta, \quad \delta \rightarrow 0, \quad (5)$$

and

$$\tilde{\sigma}_{\mu\nu}(\varepsilon_1, \varepsilon_2) = -\frac{\hbar}{\pi N_0 \Omega_{at}} \text{Tr} \langle J_\mu G(\varepsilon_1) J_\nu G(\varepsilon_2) \rangle, \quad (6)$$

$$\varepsilon_i = \varepsilon^\pm, \quad i = 1, 2.$$

Using "traditional" multiple scattering theory, in a relativistic approach the Green's function can be written⁴ in a configuration space representation as

$$\begin{aligned}
\langle \mathbf{r} | G(\varepsilon) | \mathbf{r}' \rangle &= \sum_{\Lambda \Lambda'} Z_{\Lambda}^i(\mathbf{r}_i, \varepsilon) \tau_{\Lambda \Lambda'}^{ij}(\varepsilon) Z_{\Lambda'}^j(\mathbf{r}'_j, \varepsilon)^\dagger \\
&\quad - \delta_{ij} \sum_{\Lambda} \{ R_{\Lambda}^i(\mathbf{r}_i, \varepsilon) Z_{\Lambda}^i(\mathbf{r}'_i, \varepsilon)^\dagger \Theta(r_i - r'_i) \\
&\quad + Z_{\Lambda}^i(\mathbf{r}_i, \varepsilon) R_{\Lambda}^i(\mathbf{r}'_i, \varepsilon)^\dagger \Theta(r'_i - r_i) \}, \quad (7)
\end{aligned}$$

where i and j label sites, the $Z_{\Lambda}^i(r, \varepsilon)$ and $R_{\Lambda}^i(r, \varepsilon)$, $\Lambda = (\kappa \mu)$, κ and μ being the relativistic angular quantum numbers, are properly normalized regular and irregular scattering solutions corresponding to the energy ε and the potential $V_i(R_i)$, $\mathbf{r} = \mathbf{r}_i + \mathbf{R}_i$. The matrix of the so-called scattering-path operator (SPO) is of the form

$$\boldsymbol{\tau}(\varepsilon) = \{ \tau^{ij}(\varepsilon) \}, \quad \tau^{ij}(\varepsilon) = \{ \tau_{\Lambda \Lambda'}^{ij}(\varepsilon) \}, \quad \Lambda = (\kappa \mu),$$

and so are the single-site t matrices,

$$\mathbf{t}(\varepsilon) = \{ t^i(\varepsilon) \delta_{ij} \}, \quad t^i(\varepsilon) = \{ t_{\Lambda \Lambda'}^i(\varepsilon) \},$$

and the matrix of structure constants

$$\mathbf{G}^0(\varepsilon) = \{ G^{0,ij}(\varepsilon) \}, \quad G^{0,ij}(\varepsilon) = \{ G_{\Lambda \Lambda'}^{0,ij}(\varepsilon) \},$$

satisfying the following fundamental equation

$$\boldsymbol{\tau}(\varepsilon) = [\mathbf{t}(\varepsilon)^{-1} - \mathbf{G}^0(\varepsilon)]^{-1}. \quad (8)$$

Let $J_{\mu}^i(\varepsilon_1, \varepsilon_2)$ denote the angular momentum representation of the μ th component of the current operator in a particular site i . Using a relativistic formulation for the current operator, namely $\mathbf{J} = ec\boldsymbol{\alpha}$, the elements of $J_{\mu}^i(\varepsilon_1, \varepsilon_2)$ are given by

$$J_{\mu, \Lambda \Lambda'}^i(\varepsilon_1, \varepsilon_2) = ec \int_{WS} Z_{\Lambda}^i(\mathbf{r}_i, \varepsilon_1)^\dagger \alpha_{\mu} Z_{\Lambda'}^i(\mathbf{r}_i, \varepsilon_2) d^3 r_i, \quad (9)$$

where the α_{μ} are the standard 4×4 Dirac matrices and WS denotes the volume of the Wigner-Seitz sphere.

If no translational symmetry at all is present, then in principle one has to sum over all sites in the system including leads, contacts, etc., i.e.,

$$\begin{aligned}
\tilde{\sigma}_{\mu\nu}(\varepsilon_1, \varepsilon_2) &= (C/N_0) \sum_{i=1}^{N_0} \sum_{j=1}^{N_0} \text{Tr} \langle J_{\mu}^i(\varepsilon_2, \varepsilon_1) \tau^{ij}(\varepsilon_1) \\
&\quad \times J_{\nu}^j(\varepsilon_1, \varepsilon_2) \tau^{ji}(\varepsilon_2) \rangle \quad (10)
\end{aligned}$$

with $C = -(4m^2/\hbar^3 \pi \Omega_{at})$ and $N_0 \approx 10^{23}$. As such a procedure is numerically not accessible one can define the following quantity:

$$\begin{aligned}
\tilde{\sigma}_{\mu\nu}(\varepsilon_1, \varepsilon_2; n) &= \sum_{i=1}^n \sum_{j=1}^n \tilde{\sigma}_{\mu\nu}^{ij}(\varepsilon_1, \varepsilon_2) \\
&= (C/n) \sum_{i=1}^n \sum_{j=1}^n \text{Tr} \langle J_{\mu}^i(\varepsilon_2, \varepsilon_1) \tau^{ij}(\varepsilon_1) \\
&\quad \times J_{\nu}^j(\varepsilon_1, \varepsilon_2) \tau^{ji}(\varepsilon_2) \rangle, \quad (11)
\end{aligned}$$

with n being the number of sites in a chosen region (“cluster”). This implies, however, that the convergence properties of $\tilde{\sigma}_{\mu\nu}(\varepsilon_1, \varepsilon_2; n)$ with respect to n have to be investigated. Clearly enough the most useful test cases are those where the answer is known, namely, for pure (bulk) metals or binary bulk substitutional alloys.

By using the embedded cluster method¹² for finite clusters in or on a particular substrate (host), the real space scattering path operator of an ensemble of scatterers is given by

$$\boldsymbol{\tau}_{cluster}(\varepsilon) = \boldsymbol{\tau}_{host}(\varepsilon) [\mathbf{I} - \boldsymbol{\Delta} \mathbf{t}^{-1}(\varepsilon) \boldsymbol{\tau}_{host}(\varepsilon)]^{-1}, \quad (12)$$

where $\boldsymbol{\tau}_{host}(\varepsilon)$ refers to the real-space SPO of the *two-dimensional* translational invariant host. In here, $\boldsymbol{\Delta} \mathbf{t}^{-1}$ stands for the difference of the inverse single-site t matrices for the host atoms and all atoms that form the cluster:

$$\boldsymbol{\Delta} \mathbf{t}^{-1}(\varepsilon) = \{ \boldsymbol{\Delta} \mathbf{t}_{ij}^{-1}(\varepsilon) = (\mathbf{t}_{i,host}^{-1}(\varepsilon) - \mathbf{t}_{i,cluster}^{-1}(\varepsilon)) \delta_{ij} \} \quad (13)$$

In the particular case of a substitutional binary alloy serving as host, configurational averages have to be performed,^{8,9} e.g., for the site-diagonal terms in the following manner:

$$\begin{aligned}
\langle \tilde{\sigma}_{\mu\nu}^{ii}(\varepsilon_1, \varepsilon_2) \rangle &= \sum_{\alpha} c_{\alpha} \langle \text{Tr} [J_{\mu}^{\alpha}(\varepsilon_2, \varepsilon_1) \tau^{ii}(\varepsilon_1) \\
&\quad \times J_{\nu}^{\alpha}(\varepsilon_1, \varepsilon_2) \tau^{ii}(\varepsilon_2)] \rangle_{i=\alpha}, \quad (14)
\end{aligned}$$

where c_{α} denotes the concentration of the α th component, $\alpha \in \{A, B\}$, of a binary alloy. Omitting vertex corrections this reduces to

$$\begin{aligned}
\langle \tilde{\sigma}_{\mu\nu}^{ii}(\varepsilon_1, \varepsilon_2) \rangle &= \sum_{\alpha} c_{\alpha} \text{Tr} [J_{\mu}^{\alpha}(\varepsilon_2, \varepsilon_1) \langle \tau^{ii}(\varepsilon_1) \rangle_{i=\alpha} J_{\nu}^{\alpha}(\varepsilon_1, \varepsilon_2) \\
&\quad \times \langle \tau^{ii}(\varepsilon_2) \rangle_{i=\alpha}], \quad (15)
\end{aligned}$$

and $\langle \tau^{ii}(\varepsilon) \rangle_{i=\alpha}$ can be calculated as

$$\langle \tau^{ii}(\varepsilon) \rangle_{i=\alpha} = D_{\alpha}^i(\varepsilon) \tau_c^{ii}(\varepsilon) = \tau_c^{ii}(\varepsilon) \tilde{D}_{\alpha}^i(\varepsilon), \quad (16)$$

where

$$\begin{aligned}
D_{\alpha}^i(\varepsilon) &= [I - \tau_c^{ii}(\varepsilon) \{ (t_c^i(\varepsilon))^{-1} - (t_{\alpha}^i(\varepsilon))^{-1} \}]^{-1}, \\
\tilde{D}_{\alpha}^i(\varepsilon) &= [I - \{ (t_c^i(\varepsilon))^{-1} - (t_{\alpha}^i(\varepsilon))^{-1} \} \tau_c^{ii}(\varepsilon)]^{-1}, \quad (17)
\end{aligned}$$

and τ_c^{ii} is the i th site-diagonal block of the SPO corresponding to a uniform coherent single-site t -matrix, t_c . D_{α}^i and \tilde{D}_{α}^i are the so-called impurity matrices [see Eqs. (51) and (52) of Ref. 8]. For $i=j$ one therefore gets

$$\begin{aligned}
\langle \tilde{\sigma}_{\mu\nu}^{ii}(\varepsilon_1, \varepsilon_2) \rangle &= \sum_{\alpha} c_{\alpha} \text{Tr} [J_{\mu}^{\alpha}(\varepsilon_2, \varepsilon_1) D_{\alpha}^i(\varepsilon_1) \\
&\quad \times \tau_c^{ii}(\varepsilon_1) J_{\nu}^{\alpha}(\varepsilon_1, \varepsilon_2) D_{\alpha}^i(\varepsilon_2) \tau_c^{ii}(\varepsilon_2)]. \quad (18)
\end{aligned}$$

For the $i \neq j$ case,

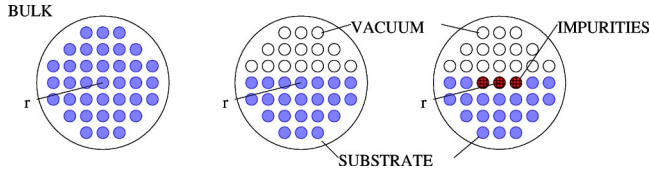


FIG. 1. Sketch of different cluster types. The entry to the left refers to bulk systems, the one in the middle to semi-infinite systems, and the one on the right to impurities embedded in the surface plane of a semi-infinite system.

$$\langle \tilde{\sigma}_{\mu\nu}^{ij}(\varepsilon_1, \varepsilon_2) \rangle = \sum_{\alpha, \beta} c_\alpha c_\beta \langle \text{Tr}[J_\mu^\alpha(\varepsilon_2, \varepsilon_1) \tau^{ij}(\varepsilon_1) \times J_\nu^\beta(\varepsilon_1, \varepsilon_2) \tau^{ji}(\varepsilon_2)] \rangle_{i=\alpha, j=\beta}; \quad (19)$$

by omitting vertex corrections this reduces to

$$\langle \tilde{\sigma}_{\mu\nu}^{ij}(\varepsilon_1, \varepsilon_2) \rangle = \sum_{\alpha, \beta} c_\alpha c_\beta \text{Tr}[J_\mu^\alpha(\varepsilon_2, \varepsilon_1) \times \langle \tau^{ij}(\varepsilon_1) \rangle_{i=\alpha, j=\beta} J_\nu^\beta(\varepsilon_1, \varepsilon_2) \times \langle \tau^{ji}(\varepsilon_2) \rangle_{i=\alpha, j=\beta}]. \quad (20)$$

Using the above defined impurity matrices, the partial averages of the SPO in Eq. (20) can be written⁸ as

$$\langle \tau^{ij}(\varepsilon_1) \rangle_{i=\alpha, j=\beta} = D_\alpha^i(\varepsilon_1) \tau_c^{ij}(\varepsilon_1) \tilde{D}_\beta^j(\varepsilon_1),$$

$$\langle \tau^{ji}(\varepsilon_2) \rangle_{i=\alpha, j=\beta} = D_\beta^j(\varepsilon_2) \tau_c^{ji}(\varepsilon_2) \tilde{D}_\alpha^i(\varepsilon_2). \quad (21)$$

Let us finally define the following expression:

$$\tilde{J}_\mu^i(\varepsilon_1, \varepsilon_2) = \sum_{\alpha} c_\alpha \tilde{D}_\alpha^i(\varepsilon_1) J_\mu^\alpha(\varepsilon_1, \varepsilon_2) D_\alpha^i(\varepsilon_2); \quad (22)$$

then, in terms of above formulas and using the properties of a trace, the contributions to the averaged nonlocal conductivity tensor between two different sites of a substitutionally disordered host are given by

$$\langle \tilde{\sigma}_{\mu\nu}^{ij}(\varepsilon_1, \varepsilon_2) \rangle = \text{Tr}[\tilde{J}_\mu^i(\varepsilon_2, \varepsilon_1) \tau_c^{ij}(\varepsilon_1) \tilde{J}_\nu^j(\varepsilon_1, \varepsilon_2) \tau_c^{ji}(\varepsilon_2)]. \quad (23)$$

COMPUTATIONAL DETAILS

For matters of convenience we define a cluster by the following set of vectors of the underlying parent lattice,¹⁴ $\mathcal{L} = \{\vec{R}_i\}$,

$$\mathcal{R} = \{\vec{R}_i \mid |\vec{R}_i^\alpha - \vec{R}_j^0| \leq r\}, \quad (24)$$

where the $\vec{R}_i^\alpha \in \mathcal{L}$ refer to either impurities sites ($\alpha = \text{imp}$), or *perturbed* host sites ($\alpha = h$), or to sites in the vacuum ($\alpha = \text{vac}$); the $\vec{R}_j^0 \in \mathcal{L}$ to *unperturbed* sites of host atoms, and r is a given length in units of the three- or two-dimensional lattice constant a_{3D} or a_{2D} of \mathcal{L} . Sketches of such clusters are displayed in Fig. 1. In the case of bulk systems r simply denotes the radius of a sphere measured from a chosen ori-

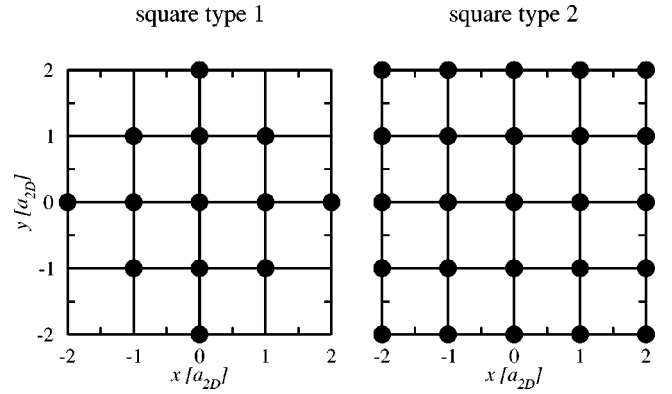


FIG. 2. Different shapes of clusters in the surface plane of a fcc(100) substrate.

gin, in the case of finite chains embedded in the surface layer of a semi-infinite host r is assumed to be one only in the self-consistent calculations.

In all cases we used potentials as calculated self-consistently for either a bulk system (fcc-Ag, fcc-Cu_xPt_{1-x}), or a free surface of a semi-infinite system⁵ [fcc-Ag(100)], or by embedding¹² a given cluster in the semi-infinite system of host atoms [finite chains of Fe and Co in the surface layer of Ag(100)].

The orientation of the magnetization is chosen to be normal to the fcc(100) plane, i.e., points along the z axis. For the angular momentum expansion we used $l_{max} = 2$. In the case of the Ag surface (fcc parent lattice, no lattice relaxation effects are included) 1830 k_{\parallel} points in the irreducible wedge of the two-dimensional Brillouin zone were used to perform the real-space host SPO calculations, in the bulk cases 630 k_{\parallel} points, in the cases of Fe and Co impurities embedded into the surface layer of Ag(100) 210 k_{\parallel} points.

If only *unperturbed* host atoms form the cluster, then by increasing the size of the cluster, the physical properties characteristic for the bulk or surface host can be expected. As a rigorous test for the proposed method we used therefore such a “self-embedding” procedure, i.e., just taking $\tau_{cluster}(\varepsilon) = \tau_{host}(\varepsilon)$ [or $\tau_{c,host}(\varepsilon)$ for a disordered system] in Eq. (12) and calculated the quantity

$$\rho_{\mu\nu} = \lim_{\delta \rightarrow 0} \rho_{\mu\nu}(r_0; \delta), \quad \rho_{\mu\nu}(r_0; \delta) = \lim_{r \rightarrow r_0} \rho_{\mu\nu}(r; \delta), \quad (25)$$

where r_0 is a sufficiently large number,

$$\rho_{\mu\nu}(r; \delta) = [\sigma_{\mu\nu}^0(r; \delta)]^{-1}, \quad \sigma_{\mu\nu}^0(r; \delta) = \sum_{|\vec{R}_{0j}| \leq r} \sigma_{\mu\nu}^{0j}(\delta), \quad (26)$$

and δ refers to the imaginary part of the Fermi energy, see Eq. (5). Performing the $\delta \rightarrow 0$ limit at the stage of Eq. (25) actually means that the side limits in Eq. (4) are taken at the last possible step.

I. SURFACE LAYER OF AG(100)

Two different squarelike shaped planar clusters were investigated (see Fig. 2), both having C_{4v} symmetry which

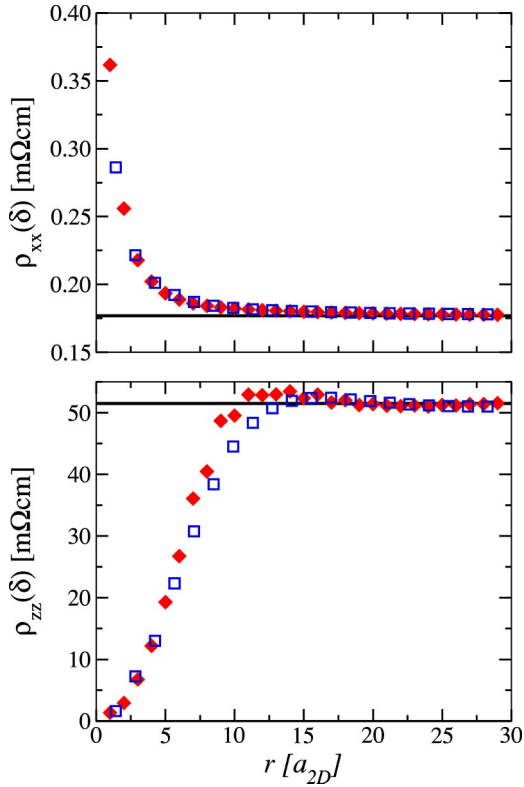


FIG. 3. Planar Ag clusters self-embedded into the surface layer of Ag(100). The in-plane (xx) and perpendicular to the plane (zz) resistivity components for two different cluster shapes are shown versus the characteristic size of the cluster (r). Diamonds correspond to type 1 in Fig. 2, squares to type 2. The horizontal line refers to the layer-diagonal resistivity (Ref. 9) as calculated using a 2D lattice Fourier transformation. δ corresponds to 1 mRy, and $a_{2D} = 5.508$ a.u.

implies the following form for $\rho_{\mu\nu}(r; \delta)$:

$$\rho_{\mu\nu}(r; \delta) = \begin{pmatrix} \rho_{xx}(r; \delta) & 0 & 0 \\ 0 & \rho_{yy}(r; \delta) & 0 \\ 0 & 0 & \rho_{zz}(r; \delta) \end{pmatrix}. \quad (27)$$

Increasing the size of the clusters we expect that $\rho_{\mu\mu}(r; \delta)$ approaches $\rho_{\mu\mu}^{pp}(\delta)$, namely, the layer-diagonal (pp) resistivity of that layer in which the clusters are embedded. The latter quantity can be calculated directly using a two-dimensional lattice Fourier transformation (see Ref. 5) and compared to the cluster results. As can be seen from Fig. 3, a reliable convergence of the resistivity can be achieved for $r > 15a_{2D}$, where a_{2D} is the two-dimensional lattice constant. It should be noted that, in particular, for the resistivity normal to the planes the visually faster convergence for clusters type 2 (also see Fig. 2) is due to the larger number of atoms forming these clusters than those of type 1.

II. BULK RESISTIVITIES

In the following we investigate three-dimensional clusters “self-embedded” into different bulk systems, such as in pure bulk metals and in statistically disordered bulk alloys, and

compare our results with known bulk resistivities (see Refs. 10 and 11). It is quite clear that for large clusters the resistivity of these clusters has to approach to the corresponding bulk value, namely to zero for pure metals and to the so-called residual resistivity for disordered alloy systems. If we assume the following behavior of the elements of the resistivity tensor with respect to the size of the cluster, given in terms of the radius of a sphere measured in units of the three-dimensional lattice constant [see Eq. (24) and Fig. 1]:

$$\rho_{\mu\mu}(r; \delta) = \rho_0(\delta) + \frac{\rho_1(\delta)}{r}, \quad (28)$$

(ρ_0 and ρ_1 are constants) it is obvious that

$$r\rho_{\mu\mu}(r; \delta) = r\rho_0(\delta) + \rho_1(\delta), \quad (29)$$

which means that the residual resistivity, $\rho_0(\delta)$ can be obtained by a linear fit of $r\rho_{\mu\mu}(r; \delta)$ with respect to r . In the case of substitutional alloys, the slope ($\rho_0(\delta)$, $\delta \rightarrow 0$) corresponds then to the residual resistivity.

A. Ag bulk

The nonvanishing elements of the nonlocal conductivity tensor ($\sigma_{\mu\nu}^{ij}$) are shown in Fig. 4, where we chose a (100)-oriented plane in the bulk with one particular atom serving as the origin of the coordinate system. It should be noted that for the out-of-plane conductivity, only scatterers are important which are not too far away from the origin, while in the in-plane case also scatterers at farther distances do add non-negligible contributions to the corresponding components of the conductivity. As can be seen, the xx and yy components are of similar form, only the shapes are rotated by 90° with respect to each other.

In principle it is sufficient to evaluate only one component of the resistivity because the system and also the clusters have cubic symmetry, which means that by choosing the coordinate system properly, all nondiagonal elements of the resistivity tensor have to be zero and the diagonal components must be identical. Deviations from this behavior can be used to estimate numerical errors inherent to the calculational scheme and the fitting procedure. The actual fitting [see Eq. (29)], was performed for each value of δ considering the last three points of $r\rho_{zz}(r; \delta)$ (Fig. 5). These points have been chosen because they refer to the biggest clusters considered (the biggest cluster contains 7935 atoms). In order to obtain the real physical residual resistivity an extrapolation to $\delta=0$ is needed; see Eq. (25). This extrapolation is illustrated in the top part of Fig. 7 and demonstrates that we made an absolute error of roughly $0.05 \mu\Omega \text{ cm}$ in our fitting procedure.

B. Cu_xPt_{1-x} bulk

More interesting than pure bulk metals are disordered bulk alloys because the accuracy of the present approach can be directly compared with experimental data and results of previous calculations. For this reason Cu_{0.50}Pt_{0.50} and Cu_{0.75}Pt_{0.25} have been chosen in order to test the reliability of

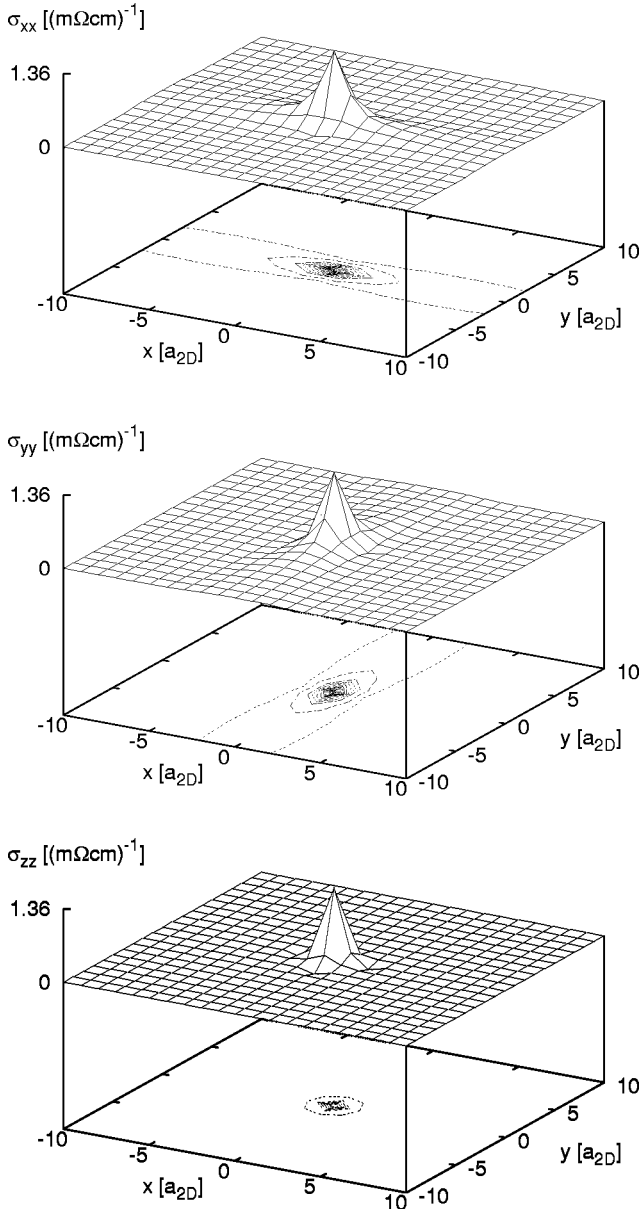


FIG. 4. Nonlocal conductivities $\sigma_{\mu\mu}^{0j}(x_j, y_j)$ for bulk fcc Ag. The atom labeled by 0 is at the position (0,0), while the position of atom j is varied in a (100)-oriented plane. (δ corresponds to 1 mRy).

the present approach. Again the fitting to a linear form has been applied to the last three points of the $r\rho_{\mu\mu}(r)$ function for each δ , in turn; see Fig. 6.

Extrapolating to $\delta=0$, we get the residual resistivity for the bulk systems shown in the lower parts of Fig. 7. As can be seen, the extrapolation can easily be performed because in the region $0 < \delta < 3$ mRy the resistivity depends linearly on δ . In comparing the present results with previous calculations and available experimental data (see, in particular, Ref. 11 for a discussion of relativistic effects in these systems), we find that there is good quantitative agreement for both concentrations of CuPt.

As already stated the numerical inaccuracy of the present approach can be seen best by evaluating the difference be-

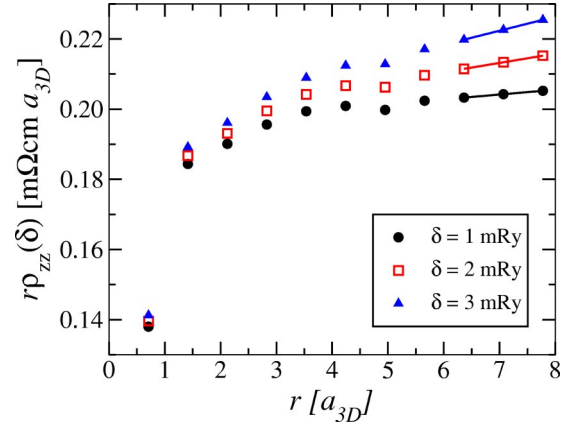


FIG. 5. Three-dimensional Ag clusters self-embedded into bulk fcc Ag. The characteristic size of the cluster (r) times the zz component of the resistivity is shown vs the size of the cluster for three different imaginary parts (δ) of the Fermi energy. ($a_{3D} = 7.78949$ a.u.).

tween the in-plane and the perpendicular to the plane elements of the residual resistivity, since the residual resistivities, ρ_{xx} and ρ_{zz} , must be the same in cubic bulk systems. It can be seen from Fig. 8 that this difference is more or less independent of δ and is of order of a few tenth of a $\mu\Omega$ cm.

It should be noted that in a fairly recent paper Dulca et al.¹³ applied real space scattering via the KKR method to the Kubo equation for bulk alloys. Although it might appear that formally their approach looks very similar to the one presented in here, fundamental conceptual differences have to be pointed out. The embedded cluster method (ECM) used by them is restricted to infinite systems [three-dimensional translational invariance, see Eq. (10) in Ref. 13], i.e., can only be used in the case of bulk systems, while in here only two-dimensional translational invariance for the substrate is

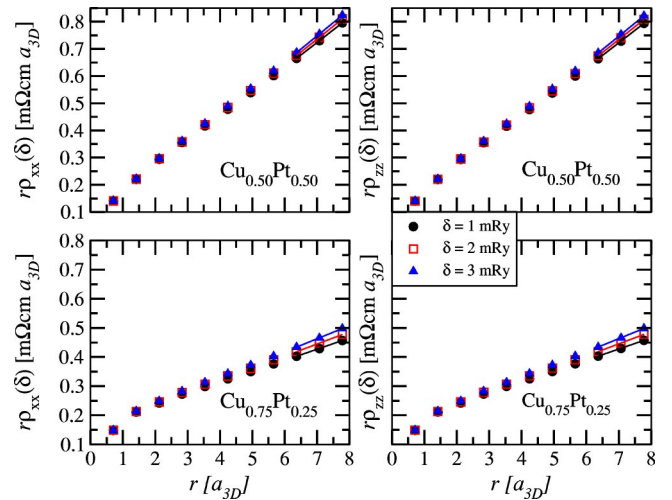


FIG. 6. Three-dimensional clusters self-embedded into disordered bulk alloys. The characteristic size of the cluster (r) times the in-plane (xx) and perpendicular to the plane (zz) resistivity components are shown versus the size of the cluster by three different imaginary parts (δ) of the Fermi energy. ($a_{3D}^{Cu_{0.50}Pt_{0.50}} = 7.14$ a.u., $a_{3D}^{Cu_{0.75}Pt_{0.25}} = 6.995$ a.u.).

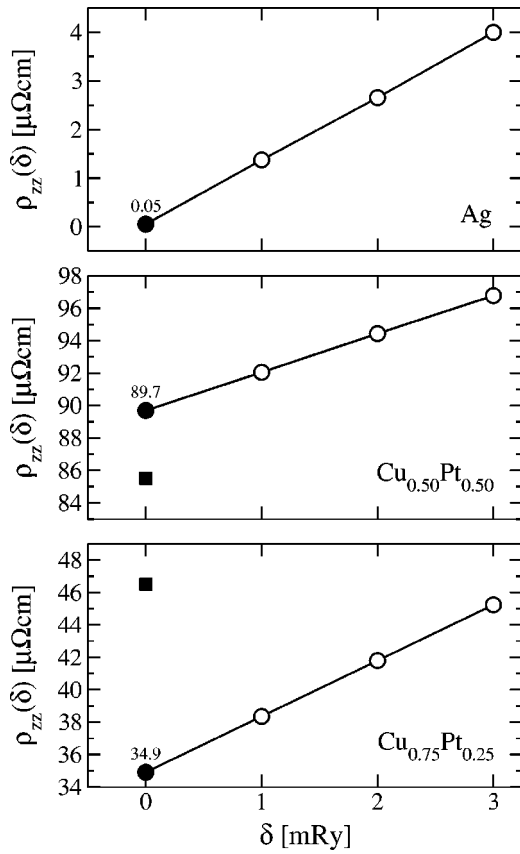


FIG. 7. Extrapolation to $\delta=0$ for the investigated bulk systems. Full circles refer to the extrapolated values and squares, to experimental values measured at room temperature (Ref. 11). The results of Dulca *et al.* (Ref. 13) are 80.2 and $31.5 \mu\Omega \text{ cm}$ for $\text{Cu}_{0.50}\text{Pt}_{0.50}$ and $\text{Cu}_{0.75}\text{Pt}_{0.25}$, respectively.

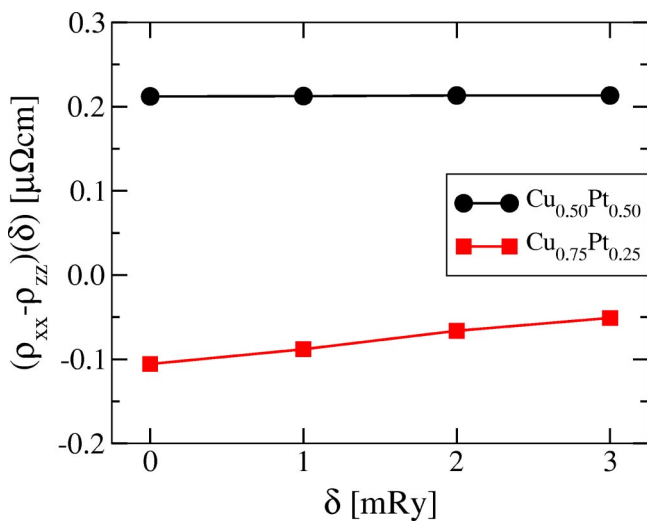


FIG. 8. Difference between the residual resistivity for the in-plane (xx) and the perpendicular to the plane (zz) component is shown vs the imaginary part (δ) of the Fermi energy for $\text{Cu}_{0.50}\text{Pt}_{0.50}$ and $\text{Cu}_{0.75}\text{Pt}_{0.25}$.

assumed, which facilitates a correct embedding into semi-infinite systems (systems with surface or interfaces). Furthermore, as stated by Dulca *et al.*¹³ their ECM necessarily is (charge) non-self-consistent, whereas in the present case for substitutional alloys serving as substrate the embedding problem is solved (charge) selfconsistently. The results shown in here for bulk systems have to be viewed entirely as an illustration of the accuracy of the present approach. The approach suggested by Dulca *et al.*¹³ is perfectly suited to discuss short-range order effects in bulk binary substitutional alloys; it cannot be used for evaluating electric properties of nanostructures in or at surfaces of semi-infinite systems.

III. NANOSTRUCTURES

As an illustration for applications in direction of nanostructures finite chains of Fe and Co embedded in the surface of Ag(100) were considered, also see Fig. 1, and Refs. 12 and 15, using the above mentioned embedded cluster method for semi-infinite systems. For this particular investigation the orientation for the magnetization was chosen to point along the surface normal (z axis).

Since clearly enough a summation over all sites including the semi-infinite substrate would yield only the resistivity of

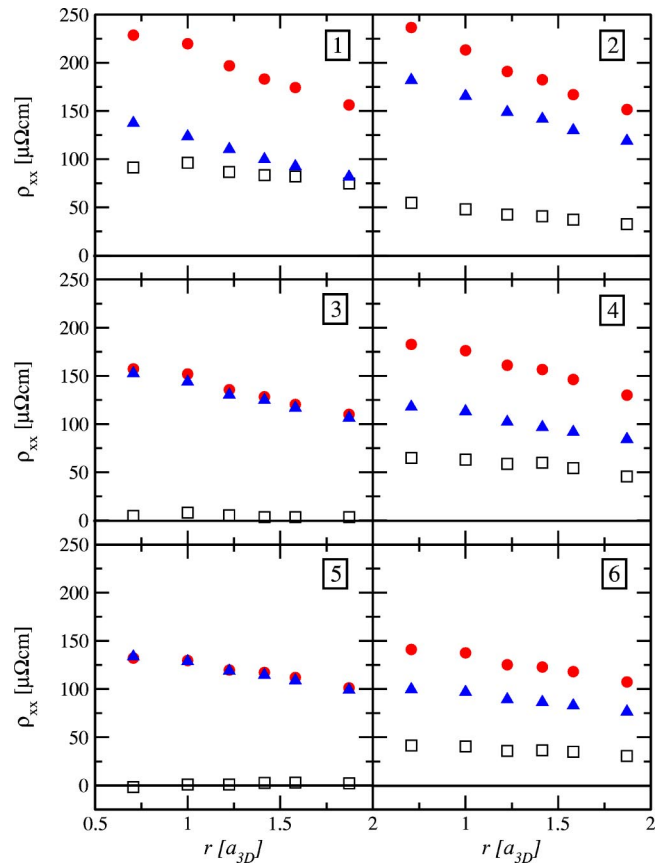


FIG. 9. Residual resistivities of finite chains of Fe (circles) and Co (triangles) atoms embedded in the surface plane of Ag(100). Open squares refer to the difference between the Fe and Co residual resistivity. The length of the chains is shown explicitly. For definitions, see the text.

the substrate, namely zero in the case of Ag(100), a kind of “residual resistivity” for finite clusters has to be defined,

$$\sigma_{\mu\mu}^{\alpha}(m;n) = \frac{1}{m} \sum_{i=1}^m \sum_{j=1}^n [\sigma_{\mu\mu}^{ij}]_{i=\alpha}, \quad (30)$$

$$\rho_{\mu\mu}^{\alpha}(m;n) = \sigma_{\mu\mu}^{\alpha}(m;n)^{-1}, \quad (31)$$

where m denotes the number of impurities of type α at sites i . The summation over the second index (j) is restricted as in the previous cases by a certain length of the difference vector \vec{R}_{ij} [see Eq. (24)], the convergence of which has to be investigated.

In Fig. 9 such residual resistivities are shown for finite chains of Fe and Co embedded along the x (110) direction in the surface layer of Ag(100). As can be seen in this figure chains with an even number of atoms differ distinctly from those with an odd number of atoms. Furthermore, for $m > 1$ and an odd chain length there is almost no difference whether Fe or Co atoms form the chains, i.e., the difference,

$$\Delta\rho_{xx}(m;n) = \rho_{xx}^{Fe}(m;n) - \rho_{xx}^{Co}(m;n), \quad (32)$$

is nearly vanishing for all n considered, whereas in the case of even chain lengths $\Delta\rho_{xx}(m;n)$ is finite and varies slowly with respect to the cluster size. For all chain lengths (m) the $\rho_{xx}^{\alpha}(m;n)$ decrease monotonically with the cluster size and can in principle again be extrapolated to large values of n by considering them as products with the cluster size.

Quite clearly at the moment no experimental data are available for such small clusters as the ones considered in here, although patterned magnetic media for recording purposes are already investigated in industrial laboratories¹⁶. Actual *ab initio* calculations of the electric properties of magnetic nanostructures will have to be performed for experimentally well-documented systems (type of substrate, type and size of nanostructures, etc.), the method of evaluation, however, has to be along the lines presented in here.

SUMMARY

By using a real-space embedding technique within the KKR Green’s function method and the CPA in combination with the real-space Kubo–Greenwood formula, we proposed a description of electrical transport properties for semi-infinite systems suitable to be applied to magnetic nanostructures. We investigated the “large cluster” limits for the Ag(100) surface, Ag bulk, and two types of CuPt bulk alloys in order to document the reliability of this approach. Good convergence to the surface resistivity was achieved by increasing the size of planar clusters, and quite reliable bulk resistivities were obtained in the case of substitutionally disordered binary alloys. Applications to finite chains of Fe and Co atoms in the surface layer of Ag(100) demonstrated the usefulness of this approach also for nanostructures. Quite clearly there are more efficient methods to evaluate resistivities for bulk or layered systems by making use of two- or three-dimensional lattice Fourier transformations. However, once it comes to determine, e.g., the electric properties of magnetic islands on surfaces, these methods are no longer applicable, and one has to rely on real space approaches as presented here.

ACKNOWLEDGMENTS

This paper resulted from a collaboration partially funded by the RTN network “Computational Magnetoelectronics” (Contract No. RTN1-1999-00145) and by the Research and Technological Cooperation Project between Austria and Hungary (Contract No. A-23/01). Financial support was also provided by the Center for Computational Materials Science (Contract No. GZ 45.451), the Austrian Science Foundation (Contract No. W004), and the Hungarian National Scientific Research Foundation (OTKA T038162 and OTKA T037856).

¹P. Grünberg, Phys. Today **54** (5), 31 (2001).

²D. J. Schiffrin, MRS Bull. **26/12**, 1015 (2001).

³L. Szunyogh, B. Újfalussy, P. Weinberger, and J. Kollár, Phys. Rev. B **49**, 2721 (1994).

⁴L. Szunyogh, B. Újfalussy, and P. Weinberger, Phys. Rev. B **51**, 9552 (1995).

⁵P. Weinberger and L. Szunyogh, Comput. Mater. Sci. **17**, 414 (2000).

⁶R. Kubo, J. Phys. Soc. Jpn. **12**, 570 (1957).

⁷D. A. Greenwood, Proc. Phys. Soc. London **71**, 585 (1958).

⁸W. H. Butler, Phys. Rev. B **31**, 3260 (1985).

⁹P. Weinberger, P. M. Levy, J. Banhart, L. Szunyogh, and B. Újfalussy, J. Phys.: Condens. Matter **8**, 7677 (1996).

¹⁰C. Blaas, P. Weinberger, L. Szunyogh, P. M. Levy, and C. B. Sommers, Phys. Rev. B **60**, 492 (1999).

¹¹J. Banhart, H. Ebert, P. Weinberger, and J. Voithländer, Phys. Rev.

B **50**, 2104 (1994).

¹²B. Lazarovits, L. Szunyogh, and P. Weinberger, Phys. Rev. B **65**, 104441 (2002).

¹³L. Dulca, J. Banhart, and G. Czycholl, Phys. Rev. B **61**, 16 502 (2000).

¹⁴P. Weinberger, Philos. Mag. B **75**, 509 (1997).

¹⁵B. Lazarovits, L. Szunyogh, and P. Weinberger, Phys. Rev. B **67**, 024415 (2003).

¹⁶G. M. McClelland, C. T. Rettner, M. Albrecht, M. W. Hart, S. Anders, T. Thomson, M. E. Best, and B. D. Terris, in *Magnetoelectronics and Magnetic Materials: Novel Phenomena and Advanced Characterization*, edited by S. Zhang, W. Kuch, G. Güntherodt, C. Broholm, A. Kent, M. R. Fitzsimmons, I. Schuller, J. B. Kortright, T. Shinjo, and Y. Zhu, MRS Symposia Proceedings No. 746 (Materials Research Society, Pittsburgh, in press).